Excited-state enhancement of optical nonlinearities in linear conjugated molecules

D. C. Rodenberger, J. R. Heflin* & A. F. Garito

Department of Physics, University of Pennsylvania, Philadelphia, Pennsylvania 19104, USA
* Present address: Department of Physics, Virginia Polytechnic Institute and State University, Blacksburg, Virginia 24061-0435, USA

NONLINEAR optical phenomena form the basis for all-optical devices such as optically bistable switches and nonlinear directional couplers[1]. The suitability of a material for these device applications requires a large magnitude of the relevant nonlinear effect (in this case, the third-order optical susceptibility $\chi^{(3)}$, which is related to the intensity-dependent refractive index) and a small signal attenuation arising from the linear optical absorption. Conjugated organic molecules and polymers are of particular interest in this context: the delocalized π-electron systems of these materials give rise to relatively large values of $\chi^{(3)}$, with extremely fast response times, in wavelength regimes where there is minimal background absorption. Previous theoretical studies[2] suggested a new enhancement mechanism for the nonlinear optical processes in these materials through population of the electronic excited states. Here we show that by optically exciting a linear conjugated molecule at one wavelength into an electronic excited state for a sufficient length of time to perform the nonlinear optical measurement, the value of $\chi^{(3)}$ can be enhanced by more than two orders of magnitude without increasing optical absorption at the probe wavelength.

An electronic nonlinear optical process is said to be nonresonant when the wavelengths involved are far from any absorbing electronic transitions. Resonant processes generally have much larger nonlinear susceptibilities, but are slower because real electronic excitations occur; they also involve considerable absorptive loss of the optical beam. Nonresonant processes, as they involve only virtual electronic excitations, are essentially instantaneous, and avoid attenuation of the optical signal. The third-order nonlinear optical susceptibility is denoted $\chi^{(3)}(-\omega_4; \omega_1, \omega_2, \omega_3)$, where $\omega_4 = (\omega_1 + \omega_2 + \omega_3)$ is the frequency of the output light in response to light input at frequencies ω_1, ω_2 and ω_3. One standard method for measurement of $\chi^{(3)}(-\omega; \omega, \omega, -\omega)$ (where the negative sign of the final frequency argument indicates that the complex conjugate of the electric field is involved in the process) is degenerate four-wave mixing (DFWM), in which two optical beams form a phase or intensity grating that modulates the refractive index of a material and a third beam scatters off the grating in an entirely new direction[3].

We have previously presented a theoretical enhancement mechanism for nonlinear optical processes originating from real population of electronic excited states in conjugated linear chains[2]. Compared with the ground state[4,5], the calculated nonresonant third-order optical susceptibility $\chi^{(3)}(-\omega_4; \omega_1, \omega_2, \omega_3)$ of π-conjugated linear chain molecules can be enhanced by orders of magnitude, or even change sign, when the first (S_1) or second (S_2) electronic excited state is optically pumped and then populated for times long enough to perform nonresonant measurements of $\chi^{(3)}(-\omega_4; \omega_1, \omega_2, \omega_3)$ at frequencies different from the resonant pump frequency.

Here we report the experimental observation of excited state enhancement of the DFWM susceptibility $\chi^{(3)}(-\omega; \omega, \omega, -\omega)$ of a linear conjugated molecule, diphenylhexatriene (DPH), when the first one-photon allowed π-electron excited state is populated for nanoseconds and then probed nonresonantly through picosecond DFWM.

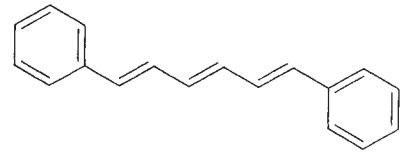

diphenylhexatriene

DPH shows saturable absorption from the $S_0(1\,^1A_g)$ ground state to the $S_2(1\,^1B_u)$ excited state centred near 350 nm, with an excited state lifetime of several nanoseconds[6,7], and is transparent at wavelengths from 400 nm to greater than 2,000 nm. Excitation to the S_2 state is known to lead additionally to population of the $S_1(2\,^1A_g)$ state, which lies at a slightly lower energy[6]. The precise assignment of excited-state population densities is irrelevant here; therefore, we refer to the excited-state population distribution hereafter simply as the S_2 state, for clarity. Fresh samples of DPH were dissolved in solutions of anhydrous dioxane, in concentrations of $1\text{-}10 \times 10^{-3}$ M, and kept isolated from atmospheric contamination.

The DFWM experiment (Fig. 1) is done using two orthogonally polarized, 1,064-nm probe beams and a 355-nm pump beam produced by a 30-ps pulsewidth, mode-locked Nd:YAG laser. The three pulsed beams, for which the relative time delays can be variably adjusted, are focused in coincidence on a thin quartz cell through which the sample solutions flow. Coherent interference of the two probes in the sample produces a refractive index grating, and the diffracted intensity of each probe from this grating, proportional to the square of the third-order optical susceptibility $\chi^{(3)}(-\omega; \omega, \omega, -\omega)$, is detected. In this DFWM arrangement there are therefore only two incident beams, rather than three[3]. The unique feature of our experimental configuration is that by introducing an intense optical pump beam tuned to the first electronic absorption band of the

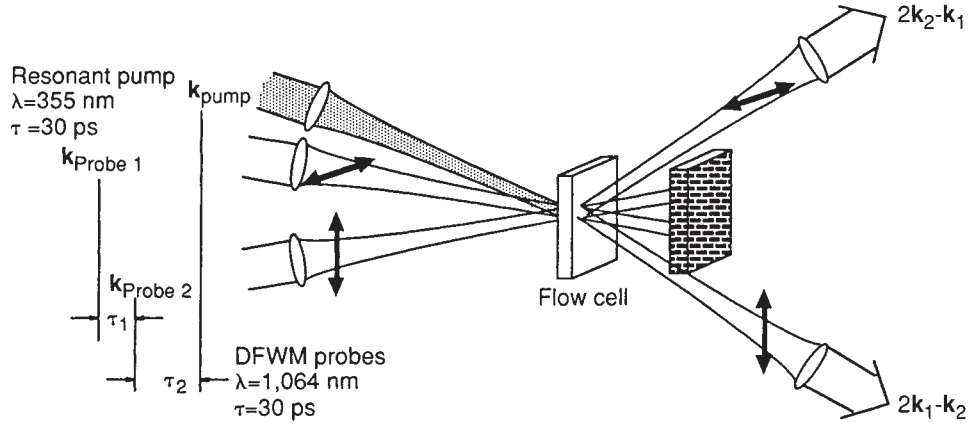

FIG. 1 Forward-scattering DFWM experiment. The $\mathbf{k}_1$ probe is horizontally polarized, the $\mathbf{k}_2$ probe is vertically polarized, and the phase-matched signal in the $2\mathbf{k}_2 - \mathbf{k}_1$ direction is detected by an infrared active photomultiplier tube following a system of apertures and a horizontally oriented analysing polarizer.

material, we force a large fraction of the molecules in the sample to occupy the first optical excited state.

An increase as large as a factor of 100 in the completely nonresonant 1,064-nm DFWM signal from the highest DPH concentrations is observed when the 355-nm pump beam saturates the S_2 absorption as compared to when the pump beam is turned off. When no pump beam is present, the ground-state molecular susceptibility $\gamma^{S_0}(-\omega;\omega,\omega,-\omega)$ of DPH and the dioxane solvent susceptibility $\gamma^{D}(-\omega;\omega,\omega,-\omega)$ contribute to the net observed macroscopic susceptibility

$$\chi^{(3)}(-\omega;\omega,\omega,-\omega) = (f^{\omega})^4[N_D\gamma^{D}(-\omega;\omega,\omega,-\omega)+N_{S_0}\gamma^{S_0}(-\omega;\omega,\omega,-\omega)]$$

where N_{S_0} and N_D are the number densities of the ground state DPH and dioxane molecules respectively, and f^{ω} is the local field factor. When the pump beam is present, however, the corresponding macroscopic susceptibility is given by

$$\chi^{(3)}(-\omega;\omega,\omega,-\omega) = (f^{\omega})^4[N_D\gamma^{D}(-\omega;\omega,\omega,-\omega)+N_{S_0}\gamma^{S_0}(-\omega;\omega,\omega,-\omega) + N_{S_2}\gamma^{S_2}(-\omega;\omega,\omega,-\omega)]$$

where N_{S_2} and γ^{S_2} are the corresponding number density and molecular susceptibility for the S_2 state. The unpumped DFWM signal is observed to be independent of concentration, demonstrating that the ground-state $\gamma^{S_0}(-\omega;\omega,\omega,-\omega)$ for DPH is smaller than the experimental resolution of $\pm 50\times10^{-36}$ e.s.u. The pumped DFWM signal, however, increases strongly with increased DPH concentration, showing that the excited state $\gamma^{S_2}(-\omega;\omega,\omega,-\omega)$ is more than two orders of magnitude larger than $\gamma^{S_0}(-\omega;\omega,\omega,-\omega)$. The measured values of $\chi^{(3)}(-\omega;\omega,\omega,-\omega)$ are linearly dependent on the concentration of the solution, as expected, and yield a value for $\gamma^{S_2}(-\omega;\omega,\omega,-\omega)$ of $12{,}000\pm1{,}700\times10^{-36}$ e.s.u. On population of the excited state, the $\gamma(-\omega;\omega,\omega,-\omega)$ of DPH at a nonresonant wavelength is greatly enhanced without introducing any optical loss.

In all measurements, the DFWM signal is non-zero only when the probe pulses temporally overlap in the sample (Fig. 2). As

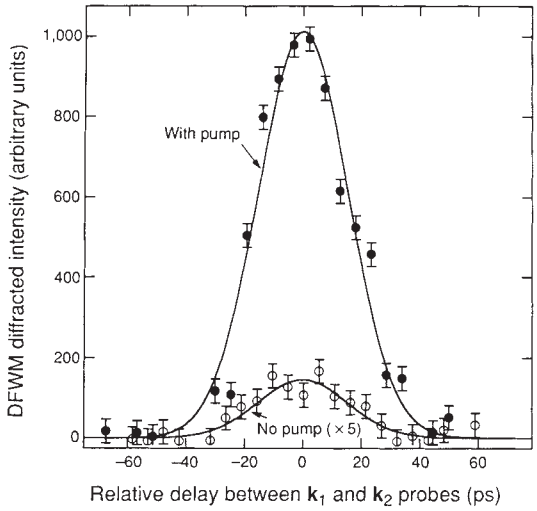

FIG. 2 Typical DFWM signal of DPH in dioxane with pump on and pump off, as a function of time delay between the two 1,064-nm probe beams. The pump delay is set so that the 355-nm pump pulse precedes the probes by 100 ps and the relative delay between the probe pulses is varied. The unpumped data, which has been multiplied by a factor of 5 for clarity, corresponds to the background signal from the dioxane solvent, because the ground-state contribution from DPH is smaller than the detection resolution of the experiment. An enhancement of a factor of 37 in intensity is shown here for a concentration of 3×10^{-3} M.

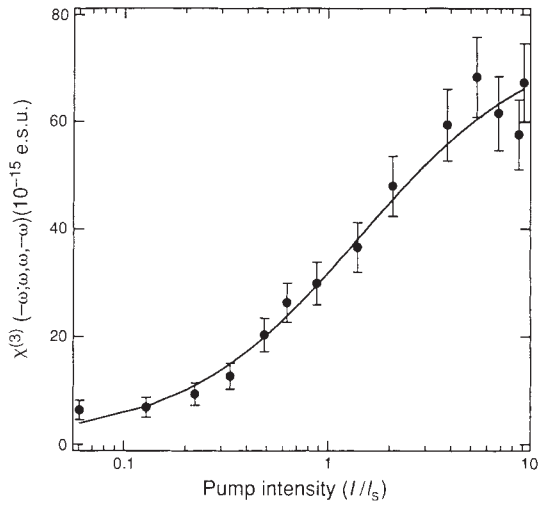

FIG. 3 Excited-state DFWM signal of DPH in dioxane as a function of pump beam intensity, demonstrating saturation. The relative delay between the probe pulses is set to zero, and the pump precedes the probes by 100 ps. At low intensity, we observe the background contribution from the dioxane solvent; at high intensity, the excited-state DPH contribution dominates.

the relative delay between the two probe pulses is adjusted, the DFWM intensity follows the expected autocorrelation of the two 30-ps pulses. Moreover, when the relative delay between the probe pulses is set to zero and the pump delay is varied, the DFWM signal shows a fast rise time followed by a nanosecond timescale decay in agreement with the probe pulsewidths and the lifetime of the S_2 state. This observed asymmetry with respect to pump pulse timing illustrates that before the pump pulse arrives, only the dioxane and DPH ground-state susceptibilities contribute, whereas at times after the pump pulse, the DPH excited-state susceptibility is detected as it decays along with the S_2 population. Additionally, the enhancement of the DFWM signal demonstrates a dependence on pump beam intensity (Fig. 3) that is in good agreement with intensity saturation of the excited-state population as found in separate saturable absorption measurements at 355 nm. Furthermore, we have done separate transient absorption experiments at 1,064 nm with excitation at 355 nm and found the excited-state absorption to be negligible.

We have observed that the DFWM signal is independent of the polarization of the pump beam, indicating that there is no coherent coupling between the pump and probes. Thus, the sole purpose of the pump beam is to create the S_2 excited-state population. The orthogonal probe polarizations ensure that the experimental DFWM signal is due entirely to the electronic third-order susceptibility of the excited state, and not due to a thermal grating. Finally, the DFWM signal is in all cases observed to have the expected cubic dependence on the probe intensities.

The enhancement mechanism demonstrated here can be generalized to second-order and other third-order nonlinear optical processes, and to other material structures, compositions and phases. The experimental observations reported here to demonstrate the principle were done on a prototype molecule with a small ground-state $\gamma^{S_0}(-\omega;\omega,\omega,-\omega)$. Furthermore, the measurements were made in solutions in which the small number density of excited state molecules with large optical nonlinearity results in a much smaller $\chi^{(3)}(-\omega;\omega,\omega,-\omega)$ than would be observed in a pure, single substance. We are currently working on pure polymer thin films where typical nonresonant ground-state values of $\chi^{(3)}(-\omega;\omega,\omega,-\omega)$ of $\sim10^{-11}$–10^{-10} e.s.u. are expected to be enhanced by several orders of magnitude, possibly leading to figures of merit sufficient for practical photonics devices. □

Received 19 June; accepted 11 August 1992.

1. Stegeman, G. I. & Stolen, R. H. *J. opt. Soc. Am.* **B6,** 652-662 (1989).
2. Zhou, Q. L., Heflin, J. R., Wong, K. Y., Zamani-Khamiri, O. & Garito, A. F. *Phys. Rev.* A**43,** 1673-1676 (1991).
3. Kobayashi, T., Terasake, A., Hattori, T. & Kurokawa, K. *Appl. Phys.* B**47,** 107-125 (1988).
4. Heflin, J. R., Cai, Y. M. & Garito, A. F. *J. opt. Soc. Am.* B**8,** 2132-2147 (1991).
5. Heflin, J. R., Wong, K. Y., Zamani-Khamiri, O. & Garito, A. F. *Phys. Rev.* B**38,** 1573-1576 (1988).
6. Kohler, B. E. & Spiglanin, T. A. *J. chem. Phys.* **82,** 2939-2941 (1985).
7. Cehelnik, E. D., Cundall, R. B., Lockwood, J. R. & Palmer, T. F. *J. phys. Chem.* **79,** 1369-1376 (1975).

ACKNOWLEDGEMENTS. This research was supported by the U.S. Air Force Office of Scientific Research, the Defense Advanced Research Project Agency, the Penn Research Fund and Pittsburgh Supercomputing Center.

Irregular glacial interstadials recorded in a new Greenland ice core

S. J. Johnsen*†, H. B. Clausen*, W. Dansgaard*, K. Fuhrer†, N. Gundestrup*, C. U. Hammer*, P. Iversen*, J. Jouzel§, B. Stauffer‡ & J. P. Steffensen*

* Geophysical Institute, University of Copenhagen, Haraldsgade 6, 2200 Copenhagen N, Denmark
† Science Institute, University of Reykjavik, Dunhaga 3, Reykjavik 107, Iceland
‡ Physikalisches Institut, Universität Bern, Sidlerstrasse 5, Bern 3012, Switzerland
§ Laboratoire de Modélisation du Climat et de l'Environment, CEA/DSM, CE Saclay 91191; and Laboratoire de Glaciologie et Géophysique de l'Environment, BP 96, 38402 St Martin d'Hères Cedex, France

THE Greenland ice sheet offers the most favourable conditions in the Northern Hemisphere for obtaining high-resolution continuous time series of climate-related parameters. Profiles of $^{18}O/^{16}O$ ratio along three previous deep Greenland ice cores[1-3] seemed to reveal irregular but well-defined episodes of relatively mild climate conditions (interstadials) during the mid and late parts of the last glaciation, but there has been some doubt as to whether the shifts in oxygen isotope ratio were genuine representations of changes in climate, rather than artefacts due to disturbed stratification. Here we present results from a new deep ice core drilled at the summit of the Greenland ice sheet, where the depositional environment and the flow pattern of the ice are close to ideal for core recovery and analysis. The results reproduce the previous findings to such a degree that the existence of the interstadial episodes can no longer be in doubt. According to a preliminary timescale based on stratigraphic studies, the interstadials lasted from 500 to 2,000 years, and their irregular occurrence suggests complexity in the behaviour of the North Atlantic ocean circulation.

Three deep Greenland ice cores, drilled from surface to bedrock at Camp Century, Dye 3 and Renland (Fig. 1) in 1966, 1981 and 1987, respectively, reach the ice deposited during the last glaciation[1-3]. This conclusion is based on the occurrence of very low $\delta^{18}O$ values ($\delta^{18}O$ is the relative deviation of the ^{18}O concentration from that in the standard mean ocean water) in the deeper parts of the cores, and on evidence that $\delta^{18}O$ in polar snow and ice depends mainly on the temperature of formation of the precipitation[4,5]. In the mid- and late glacial parts of the cores, $\delta^{18}O$ is alternately very low and intermediate (Fig. 2), corresponding to abrupt shifts between two apparently quasi-stationary climate stages[6-8]. Similar features appear in both marine[9,10] and other terrestrial records from the North Atlantic region[11,12], but only weakly in Antarctic ice cores[1,5], if at all, which points to circulation changes in the North Atlantic Ocean as the driving force[6].

Nevertheless, there has still been doubt about the climatic interpretation of the δ shifts. Intermittent occurrence of isotopically light surface meltwater in the North Atlantic Ocean was suggested as an alternative explanation of the low $\delta^{18}O$ values during the last cold period (the Younger Dryas)[13], but deuterium excess data ($d = \delta D - 8\delta^{18}O$) excluded this possibility[8]. Most recently, the meltwater peaks have been shown to coincide with the high-δ rather than the low-δ parts of the Dye 3 record (see Fig. 3*c* and *d* in ref. 14). Another suggested cause of the δ shifts at greater depths was disturbed stratification of the deeper part of the ice, as this ice has travelled a long way over a hilly bedrock[15], or, in the case of Renland, is situated only a few metres above the bedrock[3].

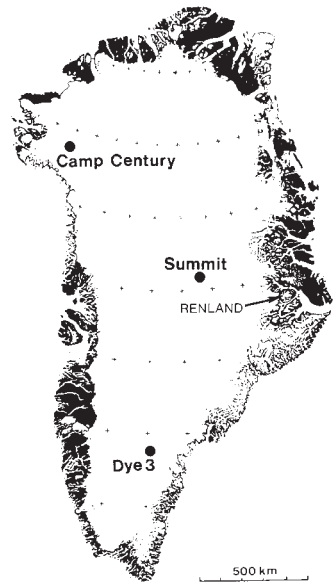

FIG. 1 Greenland with the four drill sites mentioned in the text.

The Summit location on the top of the ice sheet (Fig. 1) is an almost ideal depositional environment in which to recover an ice core: the flow pattern is simple, because there is no horizontal ice movement at present, and little in the past, when the ice divide might have been slightly displaced from its present position. Furthermore, the Summit surface temperature seldom rises above the freezing point, in contrast to Dye 3 where summer melting often causes post-depositional changes in the firn, for example absorption of additional soluble gases from the atmosphere. Summit was therefore chosen as the target of a new deep core drilling under the multinational European Greenland Ice-core Project (GRIP) 1990-1992. By the end of the second field season in 1991, the drill reached a depth of 2,321 m, where the ice is ~40,000 years old.

The timescale shown in Table 1 was established by stratigraphic methods. Back to 8,600 yr BP (before present) the timescale rests on identification of reference horizons in the form of acid volcanic fall-out dated in the Dye 3 core by counting annual $\delta^{18}O$ variations downwards from the surface[16]. Before 8,600 yr BP, the dating was accomplished by a multi-parameter method that identifies the seasonal variations of the concentrations of Ca^{2+}, microparticles, NH_4^+ and nitrate. This is extremely laborious, of course, and the resulting timescale (Table 1) is preliminary. Details will be reported elsewhere.

Figure 2 shows continuous $\delta^{18}O$ profiles along the four Greenland ice cores, plotted on linear depth scales that span the depth intervals listed in Table 2. The Summit depth scale is shown at the outer left along with the stratigraphically derived Summit timescale. The heavy and thin vertical lines indicate δ levels characteristic of low and intermediate δ, respectively.

The close correlation between the Summit and Dye 3 records rules out disturbed stratigraphy as a potential cause for the two δ levels, which must therefore be of climatic significance. Periods of relatively high δ reflect mild interstadials (IS), detectable in all four records (except for IS 3 at Camp Century). The absence